Photonic and magnetic nanoexplorers for biomedical use: from subcellular imaging to cancer diagnostics and therapy

Brian Ross[1], Alnawaz Rehemtulla[2], Yong-Eun Lee Koo[3], Ramachandra Reddy[4], Gwangseong Kim[3], Caleb Behrend[3], Sarah Buck[3], Randal J. Schneider[5], Martin A. Philbert[5], Ralph Weissleder[6], Raoul Kopelman[3*]

[1]Departments of Radiology, [2]Radiation Oncology, [3]Chemistry, and [5]Environmental Sciences, University of Michigan, Ann Arbor, MI 48109, USA; [4]Molecular Therapeutics, Inc., Ann Arbor, MI 48109, USA; [6]Center for Molecular Imaging Research, Massachusetts General Hospital, Charlestown, MA 02129,

ABSTRACT

A paradigm for brain cancer detection, treatment, and monitoring uses synergistic, multifunctional, biomedical nanoparticles for: (1) external delivery to cancer cells of singlet oxygen and reactive oxygen species (ROS), but no drugs, thus avoiding multi-drug resistance, (2) photodynamic generation of singlet oxygen and ROS by a conserved critical mass of photosensitizer, (3) enhancement of magnetic relaxivity providing for MRI contrast, (4) control of plasma residence time, (5) specific cell targeting, (6) minimized toxicity, (7) measurement of tumor kill with diffusion MRI. The 40 nm polyacrylamide nanoparticles contained Photofrin, iron-oxide (or Gd), polyethylene glycol and targeting moieties. *In-vivo* tumor growth was halted and even reversed.

Keywords: cancer detection, diffusion MRI, MRI contrast enhancement, photodynamic cancer therapy, plasma residence time, polyacrylamide nanoparticles, targeting

1. INTRODUCTION

Brain tumors, or gliomas, are among the deadliest forms of cancer, with a median life expectancy of only 6-10 months.[1] Conventional treatments such as surgical procedure, chemotherapy, and radiotherapy extend this time, but all have limited success at providing long-term cures without severe side-effects.

Photodynamic cancer therapy (PDT) is a type of light-initiated chemotherapy where a drug is activated by light, causing oxidative damage to cells, and eventually resulting in cell death. It has the promise of better selectivity and fewer side effects than radiotherapy and chemotherapy.[2-3] However, like chemotherapy, conventional PDT still suffers from the obstacle of multi-drug resistance (MDR); cancer cells pump the introduced drug molecules back out into the extra-cellular matrix.[4] Similar to radiotherapy, PDT uses locally present oxygen to produce singlet ("killer") oxygen and its oxidizing products, free radicals called reactive oxygen species (ROS), all of which destroy cancer cells.[2] In contrast to radiotherapy, which utilizes x-rays to create ROS, PDT relies on photosensitizers (PS), dyes (drugs) that produce singlet oxygen upon irradiation in the visible range. Consequently, PDT requires the tumor to be accessible to light. Brain tissue is essentially transparent to light and hence an ideal environment for PDT developmental studies.

One of the foremost and safest current imaging methods is magnetic resonance imaging (MRI). Its resolution has been improved recently by contrast enhancement agents, such as FDA approved gadolinium chelate and iron oxide nanoparticles.

Microparticles and nanoparticles can be used for drug delivery[5,6], however these are made for the eventual *release* of small drug molecules, either outside or inside the cell. These nanoparticles often are coated with PEG (polyethylene glycol), which prevents aggregation and attack by the immune system (i.e. macrophage). The PEG chain-length controls the plasma residence time of the nanoparticles. Other recent work describes nanoparticles containing PDT agents but without inclusion of MRI enhancing agents or surface modification.[7-9]

In this work we describe a new class of nanoparticles that combines the MRI contrast enhancement with targeted PDT, enabling protocols of simultaneous cancer detection, therapy and monitoring.

Nanobiophotonics and Biomedical Applications, edited by Alexander N. Cartwright,
Proc. of SPIE Vol. 5331 (SPIE, Bellingham, WA, 2004) · 1605-7422/04/$15 · doi: 10.1117/12.537653

2. DESIGN AND SYNTHESIS OF NANOPARTICLES

The particle has a polyacrylamide (PAA) core containing photosensitizers and MRI contrast agents, with a surface-coating consisting of both polyethylene glycol (PEG) and molecular targeting groups for controllable particle residence time and the recognition of the tumor neovasculature, respectively (Fig. 1A). The design of the nanoparticle is universal, flexible and allows for facile interchange of its active components, including its targeting ligands that provide control of tumor specificity. PAA nanoparticles have been used previously as optochemical sensors called PEBBLEs (Probes Encapsulated By Biologically Localized Embedding) and the technology is now being expanded for the detection and therapy of cancer. The production of polyacrylamide nanoparticles is based on the nanoemulsion techniques studied by Daubresse, et al.[10]. The photosensitizer and MRI contrast agent are introduced into the polymerization solution during nanoparticle synthesis and entrapped in the matrix pores; PEG is attached to the surface after particle formation. For the work described here, Photofrin, an FDA approved PDT agent was used as the photosensitizer and iron oxide was used as the MRI contrast agent. We note that the nanoparticle ingredients (Photofrin, gadolinium chelate/iron oxide, polyacrylamide and PEG) are all FDA approved.

The toxicity of the PAA nanoparticles was evaluated by clinical chemistry and histopathology methods. Tissues and blood were collected 3, 7 and 28 days after injection of nanoparticles to rats via the caudal vein using a flexible cannula coupled to an automated injection system (Harvard Apparatus). Sera were separated at the time of collection analyzed using a COBAS FARA II fast centrifugal automated enzyme analyzer (Roche Diagnostics). Tissues were fixed in situ by perfusion through the heart with buffered formalin and processed in a Citadel 2000-Tissue Processor (Shandon) embedded using a histocentre-2, (Shandon) sectioned (5 µm), stained (Haematoxylin and Eosin) and analyzed by light microscopy. No sign of toxicity due to the nanoparticles were found over four weeks.

The morphology of the nanoparticles was determined by SEM or multi-angle light scattering (Wyatt Technologies Corp. Santa Barbara, CA) (Fig. 1B). The average size of PAA nanoparticles used in this study ranges from 30 to 60 nm (Fig. 1C).

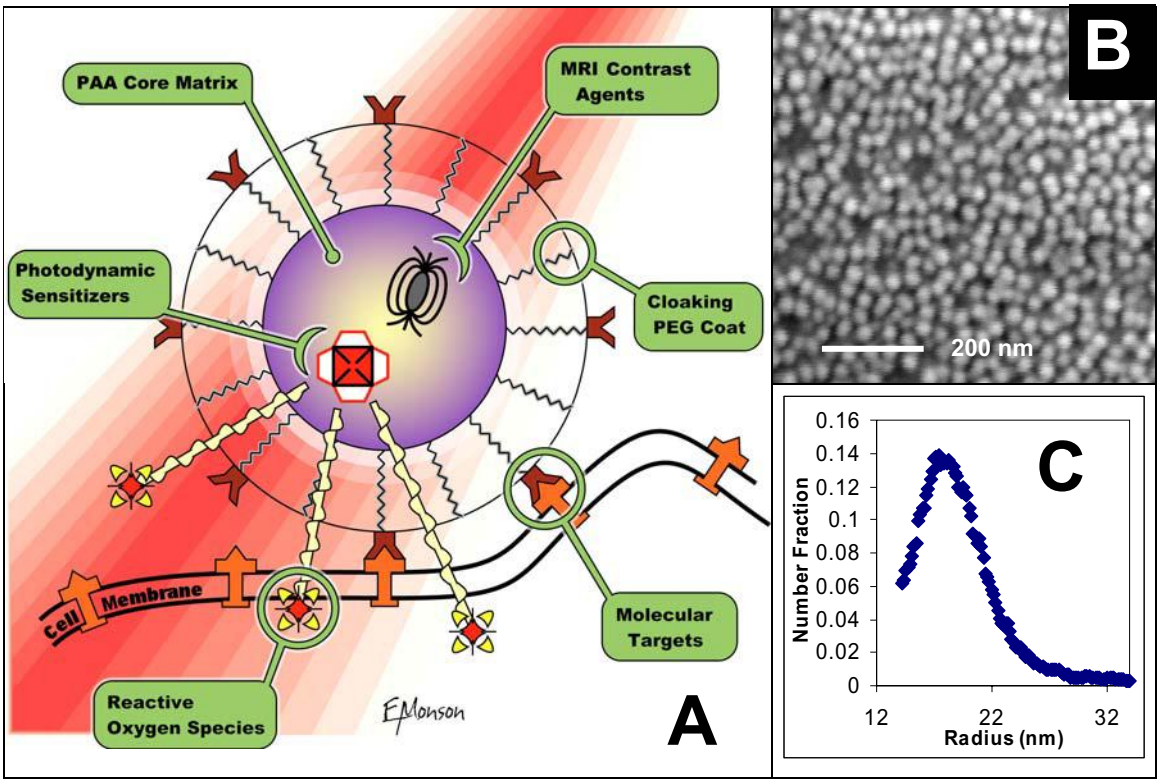

Fig. 1. Overview of Nanoparticle Platform. (**A**) Schematic Nano-platform with photodynamic dye, MRI contrast enhancement agent, polyethylene glycol (PEG) cloaking and molecular targeting. (**B**) A typical SEM image of PAA particles. (**C**) A typical size distribution result from multi-angle light scattering.

3. MAGNETIC CONTRAST ENHANCEMENT

3.1 *In vitro* MRI

In-vitro relaxivity of the iron oxide containing PAA nanoparticles was determined by MRI relaxation studies. The nanoparticle suspension of 8 mg/ml in deionized water was placed in a tube and imaged within a single field of view using a 12 cm bore, 7 tesla Varian animal system (Varian Inc., Palo Alto, CA). The measured transverse relaxation rate (R_2) was 600-770 $s^{-1}mM^{-1}$, which is approximately 5-fold greater than for other superparamagnetic iron oxide.[11]

3.2 *In vivo* MRI and Pharmacokinetics study

In-vivo MR imaging of these nanoparticles was performed after tail vein injection into a rat bearing an intracerebral 9L tumor at a dose of about 200mg/kg of body weight as a suspension (approx. 40 mg/ml) in normal saline. MR images were obtained using dynamic T_2* weighted gradient echo MRI before and after the injection, revealing significant contrast changes (Fig. 2, A to E).

The contrast changes in the images were monitored with time and further utilized for the dynamic MRI derived pharmacokinetics study on nanoparticles. Regions of interest (e.g. normal brain, muscle, tumor, vasculature etc.) were selected from the images to determine if there was a change in contrast, compared to untreated animals. This revealed a detailed picture of the pharmacokinetics of the nanoparticles. Two kinds of nanoparticles were used: non-PEGylated PAA nanoparticles and PEGylated PAA nanoparticles, with PEG of molecular weight 2 kD. The plasma half-life of non-PEGylated nanoparticles is less than 1 minute while that of PEGylated nanoparticles is longer than 2 hours (Fig. 2, F and G). This indicates that PEGylation increases the plasma half-life of the nanoparticles and can be used to control the *in-vivo* clearance of particles.

4. PDT

4.1 Chemical test for singlet oxygen production

The efficacy of the PAA nanoparticles as PDT agents depends on the production of singlet oxygen. Therefore, it is important to confirm the production of singlet oxygen from the Photofrin containing nanoparticles. This was demonstrated by both *in-vitro* cell kill and chemical tests. Anthracene-9,10-dipropionic acid, disodium salt (ADPA) was used as a singlet oxygen detection probe for the chemical test.[12] The fluorescence intensity of ADPA decays due to chemical reaction between ADPA and the singlet oxygen produced from the illuminated Photofrin inside the PAA nanoparticles (Fig. 3A).

4.2 *In vitro* cell kill

In-vitro evaluation of the nanoparticles for photodynamic therapy was done using 9L rat gliosarcoma cells, treated with various concentrations of Photofrin-containing nanoparticles (or no particles as a control) and irradiated with a laser source (Diomed 630 PDT Class IV diode laser (630 ± 3 nm)) for 5 min by at various intensities (or no light as a control). These treated (or mock treated) samples contained propidium iodide and calcein acetoxymethylester dyes to monitor dead and live cells, respectively, with a fluorescent microscope. The cell images under the four different conditions are shown in Fig. 3, B to I. In the absence of nanoparticles containing Photofrin, there was no toxicity after irradiation with the laser light. Increasing the concentration of PDT nanoparticles resulted in an increasing degree of cell death; a minimum particle concentration of 350 μg/ml was required to produce a recognizable effect under these conditions.

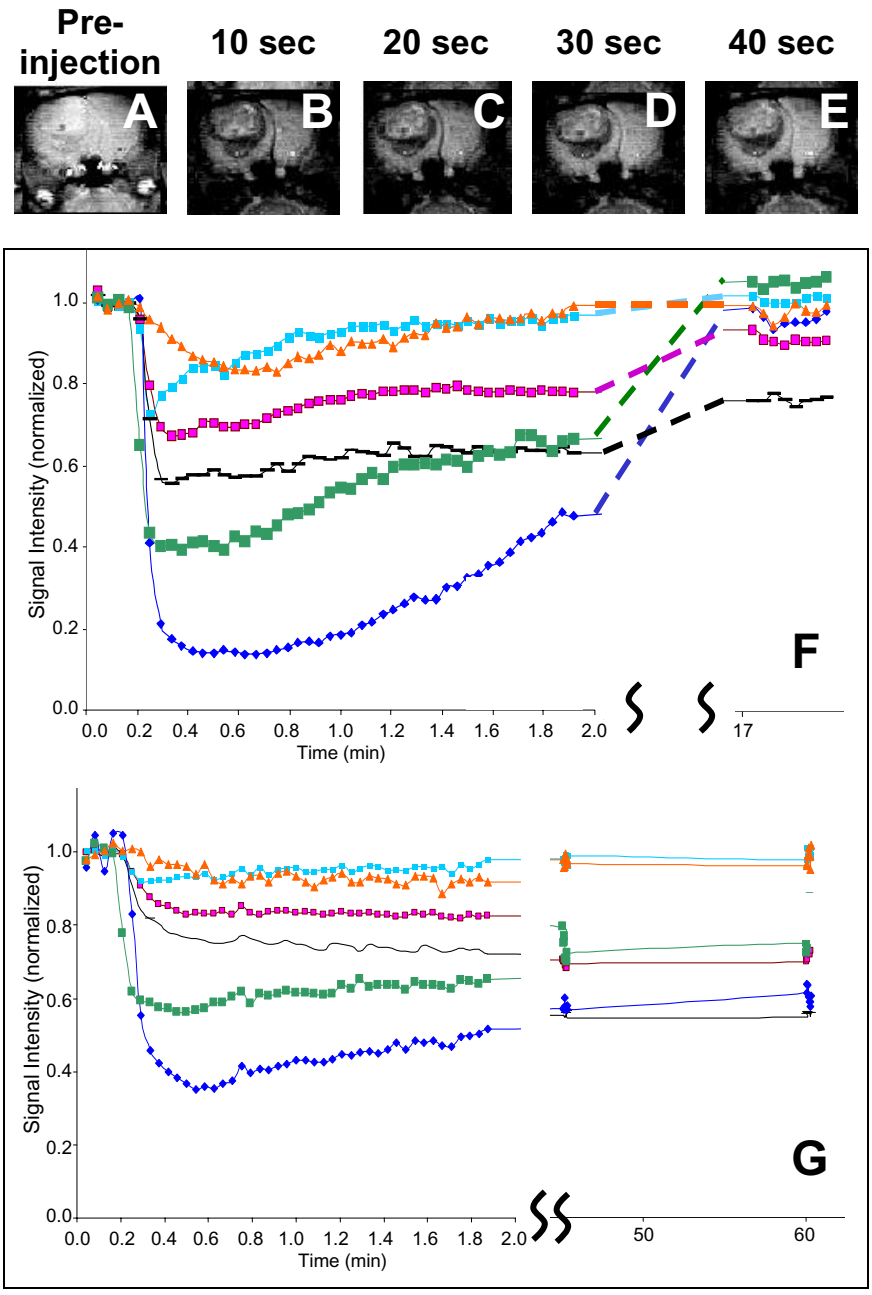

Fig. 2. MRI contrast Enhancement.
(**A** to **E**) *In-vivo* images of the rat brain by Dynamic MRI scanning. A tumor bearing rat was injected with iron oxide containing particles at a dose of about 200mg/kg of body weight and T_2^* scanning was performed every 2.5 sec. The images shown are T_2^* - weighted MR images acquired (A) prior to and (B) 10, (C) 20, (D) 30 and (E) 40 sec following *intravenous* administration.;
(**F** to **G**) Dynamic MRI derived pharmacokinetics of (F) non-PEGylated particles and (G) PEGylated particles**.** The MRI data shown in (A-E) were used to determine the presence of contrast-altering nanoparticles in each of the tissues over time (■ Tumor Core, ■ Brain, ─ Tumor Margin, ▲ Vein, ■ Artery, and ▲ Muscle).

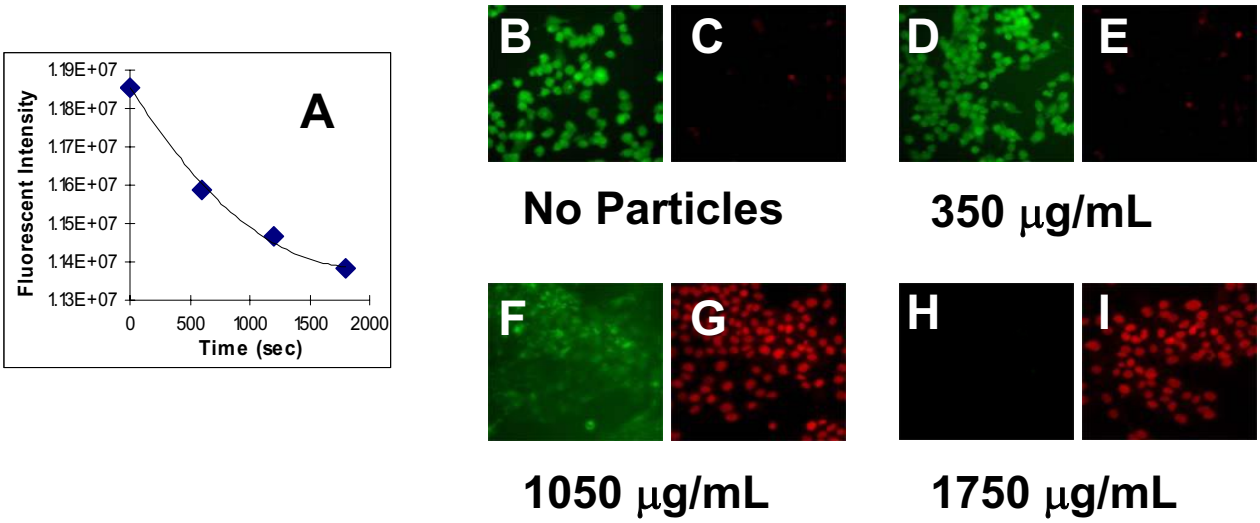

Fig. 3. Detection of Singlet Oxygen produced from Photofrin containing nanoparticles. (**A**) Decay of fluorescence intensity of ADPA in solution from chemical quenching by the singlet oxygen produced by the light-activated Photofrin inside the PAA nanoparticles. This decay is a measure of singlet oxygen production and delivery by the nanoparticles. Different wavelengths are used for the excitation of Photofrin (630 nm) and of ADPA (376 nm); (**B** to **I**) *In-vitro* cell kill tests: dose response of Photofrin nanoparticles on cultured 9L cells. (B) Living and (C) dead cells, 5 min. 1500mW laser exposure, no nanoparticles present. (D) Living and (E) dead cells, 5 min. 1500mW laser exposure, 350 μg/mL nanoparticles present. (F) Living and (G) dead cells, 5 min. 1500mW laser exposure, 1050 μg/mL nanoparticles present. (H) Living and (I) dead cells, 5 min. 1500mW laser exposure, 1750 μg/mL nanoparticles present.

4.3 *In vivo* PDT

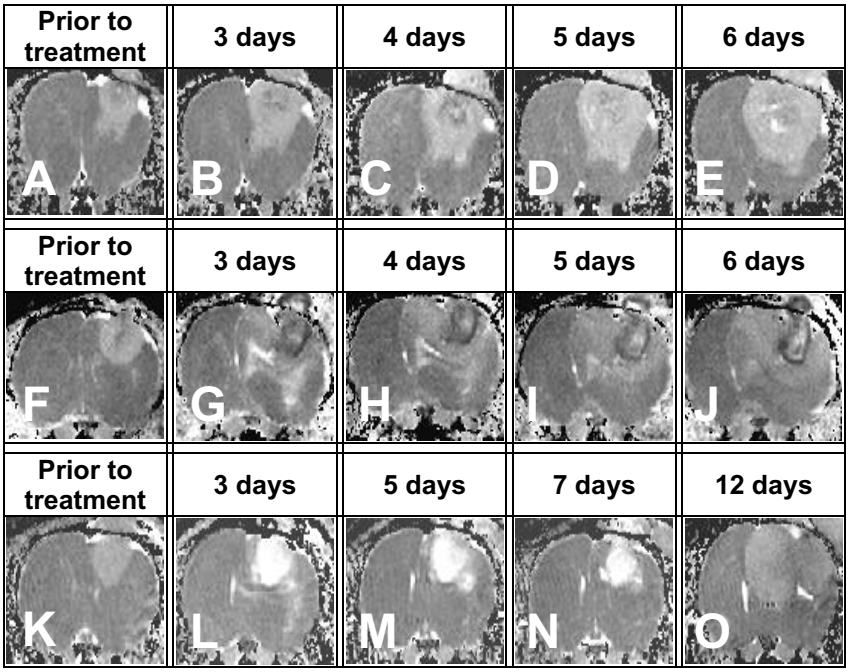

Fig. 4. *In-vivo* PDT by Photofrin containing nanoparticles: Time series of diffusion-weighted MRI of tumors
(A to E) Untreated; (F to J) Treated with light alone; (K to O) Treated with Photofrin-containing PAA nanoparticle treatment. Note the slight dark region (G to J) due to minor intratumoral hemorrhage. The huge "bright" regions reveal a significant area of necrosis resulting from the therapeutic effect. Each series of images (A to O) is from a representative animal from a group of three.

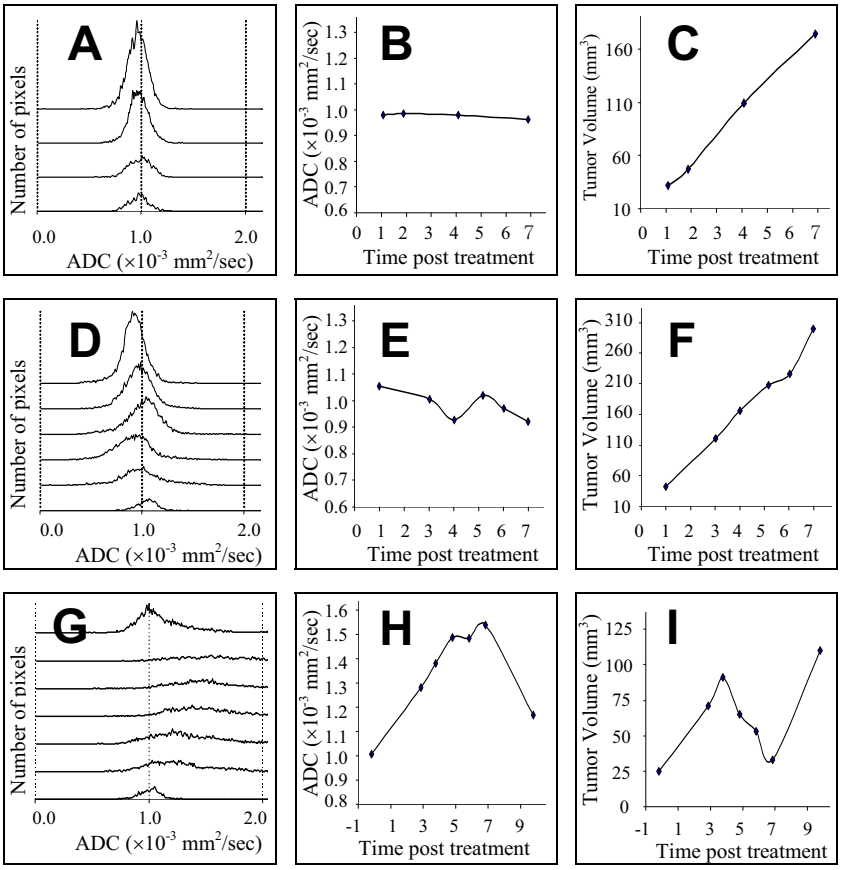

Fig. 5. Quantitative Analysis of *In-vivo* PDT by [(A), (D), and (G)] diffusion histograms mean, [(B), (E), and (H)] ADC and [(C), (F), (I)] tumor volume over time. (A to C) Untreated tumor. (D to F) Laser light treatment only. (G to I) Photofrin PAA nanoparticles and laser light treatment. Each set (A to I) reveals the data for a representative animal from a group of five.

The *in-vivo* therapeutic activity of the nanoparticles containing Photofrin was also evaluated. Rats bearing intracerebral 9L tumors were anesthetized and 1.0 ml of a 75 mg/ml (in 0.9% NaCl solution) of Photofrin nanoparticles was delivered to the rats by intravenous injection via the tail vein. After approximately 60 minutes, laser treatment was applied for 5 minutes at 700 mW using a fiber optic probe and a Diomed 630 PDT Class IV diode laser (630 ± 3 nm). The rats were then diffusion MR imaged at various time points, to monitor changes in tumor diffusion, tumor growth and tumor load. For control experiments, untreated tumor bearing rats and those with laser treatment only (for 7.5 min at 700 mW) were also monitored by diffusion MRI. The diffusion-weighted MRI can provide a more quantitative assessment of the tumor than MRI, by providing the molecular diffusion coefficients in tissue. The brightness of the voxel (volume equivalent to pixel) on each image is proportional to the mobility of the water within that tissue region. In general, the increase in tumor diffusion values corresponds to a loss of tumor cellularity within the region under study.

The time series of diffusion-weighted MR images (Fig. 4, A to O) show that the untreated 9L gliomas (Fig. 4, A to E), as well as those with laser treatment (Fig. 4A, F to J) only, continued to grow over the lifespan of the animals. However, gliomas treated by the administration of Photofrin-containing nanoparticles (Fig. 4, K to O), followed by laser irradiation, produced massive regional necrosis, resulting in shrinkage of the tumor mass. Re-growth occurred at 12 days post-treatment. The diffusion histograms were constructed based on the images and the changes in the mean apparent diffusion coefficient (ADC) and tumor volume were analyzed (Fig. 5, A to I). For untreated 9L tumors (Fig. 5, A to C), the overall distribution of diffusion values did not change, nor did the mean diffusion values, while the tumors continued to rapidly and exponentially grow over time. The treatment of tumors with laser light only did not significantly affect the overall distribution of diffusion values, nor did the mean diffusion values change while the tumors continued to grow exponentially over time (Fig. 5, D to F), indicating that exposure of the tumor to the fiber optic light source did not affect the tumor growth rates or cause sufficient damage to change tumor water diffusion values. The diffusion histograms for 9L tumors that received PDT treatment using Photofrin-containing nanoparticles

(Fig. 5, G to I) reveal that this treatment significantly increased the tumor diffusion values, as evidenced by a dramatic right-shift of the histograms. Moreover, ADC was also markedly increased following treatment, which indicates a massive cell killing effect due to this treatment approach. The increase in diffusion is correlated with significant tumor growth retardation and, in many cases, with tumor mass shrinkage. When all data are considered, it can be determined that administration of Photofrin-containing nanoparticles, followed by light activation, is a viable therapeutic approach for the treatment of brain tumors and that the therapy can be successfully monitored with a noninvasive imaging technique.

5. TARGETING

The MRI and PDT results indicate a compromised blood-brain barrier, which allows the successful localization of the untargeted nanoparticles in the tumor. However, delivery of a therapeutic agent in a targeted manner would be of great value as it has the potential to improve efficacy by increasing the amount of therapeutic agent delivered to the site thus minimizing toxicity by reducing systemic exposure.

Since expression of $\alpha_V\beta_3$ integrins is a common feature of tumor vasculatures, we have developed nanoparticles containing an RGD peptide (cyclic CDC**RGD**CFC, an $\alpha_V\beta_3$ ligand) on the surface. To enable fluorescent detection of the targeted PAA nanoparticles, Alexafluor 594 dye was included in the particle matrix. The RGD peptide was synthesized[13] and attached on the surface of an amine functionalized particle, using a sandwich of biotin and sulfosuccinimidyl 4-[*N*-maleimidomethyl] cyclohexane-1-carboxylate.

To test if the surface-modified nanoparticles selectively target tumor tissue, as compared to the unmodified nanoparticles, we introduced both kinds of particles to MDA-435 cells ($\alpha_V\beta_3$ expressing). The RGD-coated particles specifically bound to MDA-435 cells but not to MCF-7 cells ($\alpha_V\beta_3$ non-expressing) (Fig. 6). These results indicate that this particle retains the ability to specifically bind to $\alpha_V\beta_3$ expressing cells, thus enabling the targeted delivery of these particles for imaging and therapy.

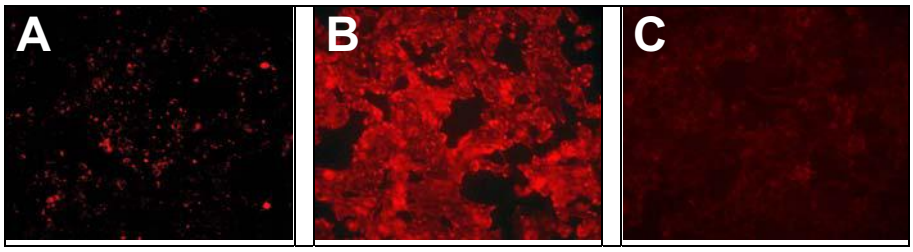

Fig. 6. RGD Targeting of fluorescent nanoparticles to cell surface receptors on viable tumor cells. MDA-435 cells were used as a positive control and MCF-7 cells were used as a negative control. (**A**) To control for non-specific binding, non-targeted PAA-nanoparticles were used with MDA 435 cells. (**B**) RGD-modified nanoparticles selectively bind to MDA-435 cells. (**C**) RGD-modified nanoparticles do not bind MCF-7 cells.

6. CONCLUSIONS

In conclusion, a multifunctional nanoparticle platform was designed and constructed for early *in-vivo* detection, therapy, and MRI monitoring of cancer. Photosensitizer and magnetic contrast agents were encapsulated and conserved within the nanoparticle core shell, still showing effective *in-vitro* and *in-vivo* tumor killing as well as drastic magnetic contrast enhancement. Because the nanoparticles do not release drugs, in contrast to conventional PDT, the stumbling block of multi-drug resistance is avoided. The entire nanoparticle acts as a large photosensitizer, delivering a high dose of singlet oxygen to the cell membrane. Active photodynamic dye molecules are not depleted, because they remain intact inside the nanoparticle, in the immediate vicinity of the cell. The overall effect is a high probability of tumor cell kill. Finally, the *in-vivo* tests (rat 9L gliosarcoma model) show the dissolution of the brain tumor upon only 5 minutes of the red light therapy administered to the rat. The MRI contrast enhancing molecules or nanocrystals are also conserved inside the core. In addition, the tumor kill is not only effective but is also quickly established by the increased

mobility (diffusivity) of its water molecules, monitored instantly or simultaneously by spatially resolved magnetic resonance. Also, the plasma residence time of the nanoparticles is controlled by the PEG. *In-vitro* tests confirm that surface-modified nanoparticles effectively target tumor related tissue for more tumor-specific delivery of therapeutic agents. Furthermore, our *in-vivo* tests show no toxic effects over four weeks. All these data show that this nanoparticle approach is a valid paradigm for cancer detection and therapy, which is flexible in its formulation and versatile in its use.

ACKNOWLEDGEMENTS

We thank Dr. Eric Monson for his help and the University of Michigan Electron Microbeam Analysis Laboratory for use of the SEM. This research was supported by NCI Contract N01-CO-07013 and N01-CO-37123.

REFERENCES

1. J. C. W. Kiwit, F. W. Floeth and W. J. Bock, "Survival in malignant glioma: Analysis of prognostic factors with special regard to cytoreductive surgery", Zbl. Neurochir. **57**, 76-88, 1996.
2. T. J. Dougherty, "An update on photodynamic therapy applications", J. Clin. Laser Med. Sur. **20**, 3-7, 2002.
3. W. Stummer, A. Hassan, O. Kempski and C. Goetz, "Photodynamic therapy within edematous brain tissue: Considerations on sensitizer dose and time point of laser irradiation", J. Photochem. Photobiol. B-Biol. **36**, 179-181, 1996.
4. G. Singh*, et al.*, "Resistance to Photodynamic Therapy in Radiation-Induced Fibrosarcoma-1 and Chinese-Hamster Ovary-Multi-Drug Resistant Cells-Invitro", Photochem. Photobiol. **54**, 307-312, 1991.
5. M. L. T. Zweers, D. W. Grijpma, G. H. M. Engbers and J. Feijen, "The preparation of monodisperse biodegradable polyester nanoparticles with a controlled size", J. Biomed. Mater. Res. Part B-Appl.Biomater. **66B**, 559-566, 2003.
6. E. Allemann, R. Gurny and E. Doelker, "Drug-Loaded Nanoparticles - Preparation Methods and Drug Targeting Issues", European J. Pharm. Biopharm. **39**, 173-191, 1993.
7. J. A. Harrell and R. Kopelman, "Biocompatible Probes measure Intracellular Activity", Biophotonics International **7(2)**, 22-24, March 2000.
8. I. Roy*, et al.*, "Ceramic-based nanoparticles entrapping water-insoluble photosensitizing anticancer drugs: A novel drug-carrier system for photodynamic therapy" J. Amer. Chem. Soc.**125**, 7860-7865, 2003.
9. H. Xu, thesis, *Sol-Gel and Polyacrylamide Based Optical Pebble Nanosensors for Intracellular Imaging and Analysis of Oxygen and Glucose*, University of Michigan (2003).
10. C. Daubresse, C. Grandfils, R. Jerome and P. Teyssie, "Enzyme Immobilization in Nanoparticles Produced by Inverse Microemulsion Polymerization", J. Colloid Interf. Sci. **168**, 222-229, 1994.
11. Y. X. J. Wang, S. M. Hussain and G. P. Krestin, "Superparamagnetic iron oxide contrast agents: physicochemical characteristics and applications in MR imaging", Eur. Radiol. **11**, 2319-2331, 2001.
12. M.J. Moreno, E. Monson, R.G. Reddy, A. Rehemtulla, B.D. Ross, M. Philbert, R.J. Schneider and R. Kopelman, "Production of Singlet Oxygen by $Ru(dpp(SO_3)_2)_3$ Incorporated in Polyacrylamide PEBBLEs", Sensors and Actuators B: Chemical, **90**, 82-89, 2003.
13. H. M. Ellerby*, et al.*, "Anti-cancer activity of targeted pro-apoptotic peptides", Nat. Med. **5**, 1032-1038, 1999.